Imaging the continuous spectrum of therapeutic radionuclides with detectors and pinholes suited for high energy

Stefaan Vandenberghe

ELIS Department, MEDISIP,
Ghent University-iMinds-IBiTech, Ghent, Belgium

Stefaan.Vandenberghe@ugent.be

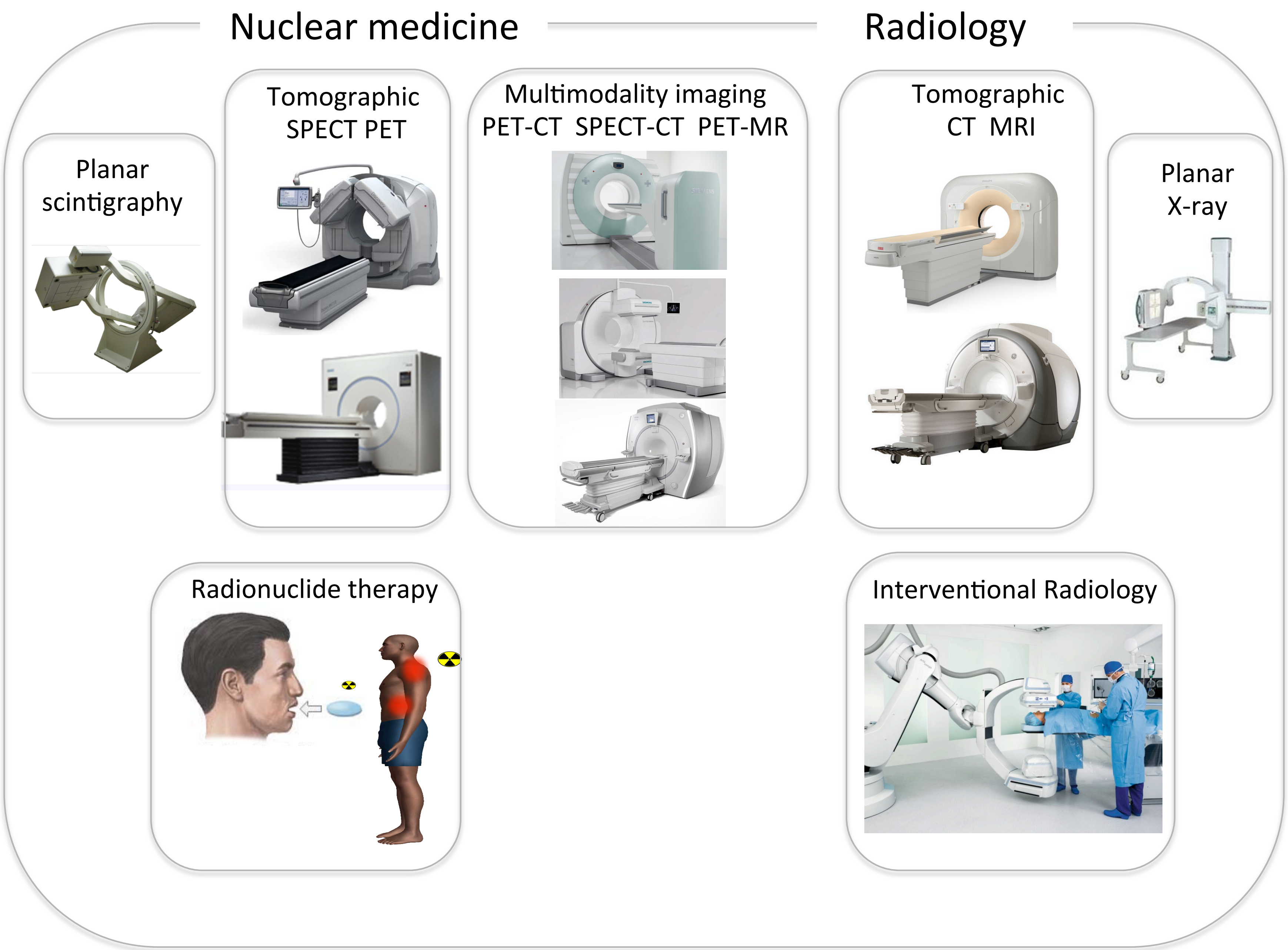
Nuclear medicine
Radiology
Planar scintigraphy
Tomographic SPECT PET
Multimodality imaging PET-CT SPECT-CT PET-MR
Tomographic CT MRI
Planar X-ray
Radionuclide therapy
Interventional Radiology

Radionuclide therapy

Applications

Thyroid I-131

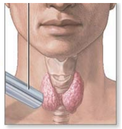

Liver tumor radioembolisation with Y-90

Neuroendocrine tumors

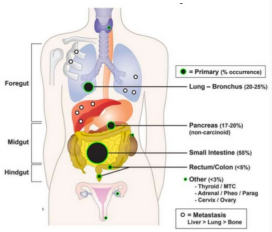

Bone tumors

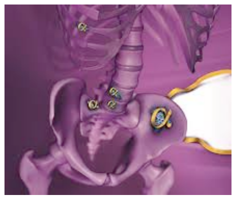

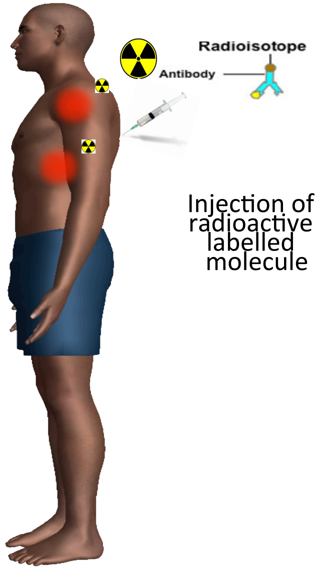

Radionuclide therapy

=

Radiation from inside

External beam therapy

=

Radiation from outside

Patient dosimetry required for individualised treatment

How to Calculate dose in radionuclide therapy?

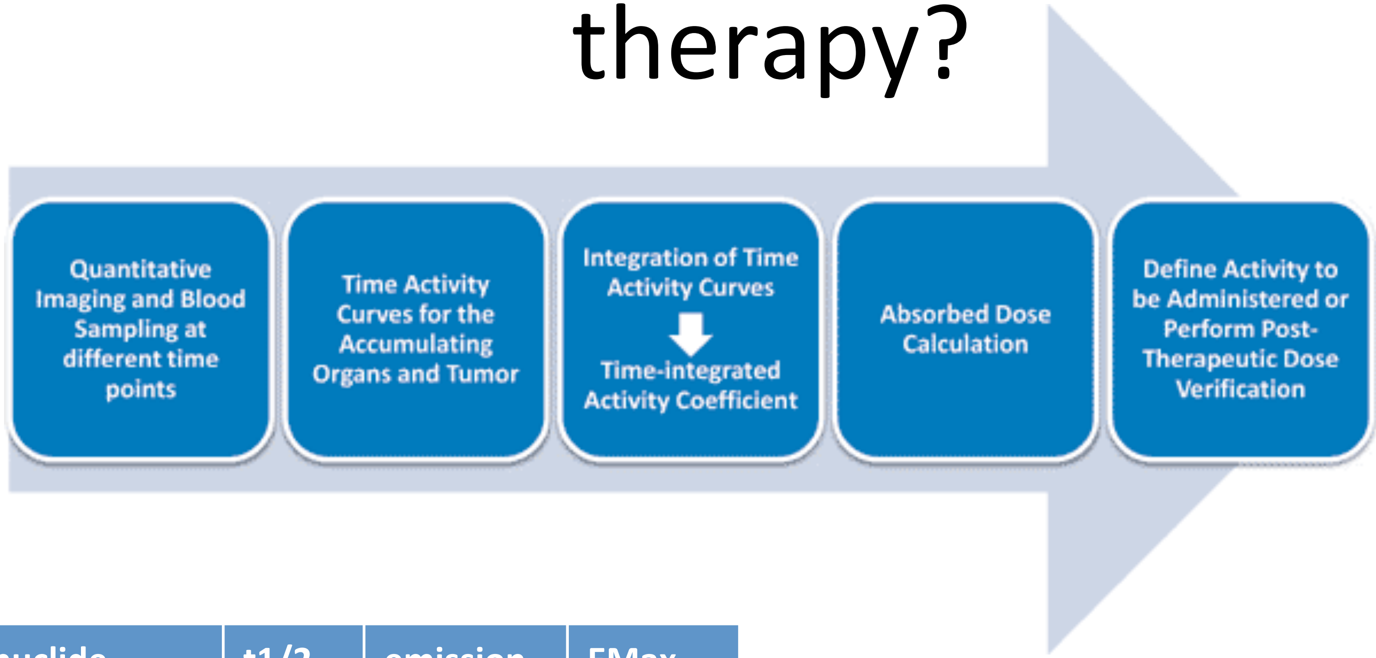

Radionuclide		t1/2	emission	EMax
I-131	Iodine	8d	Beta Gamma	606KeV 365 KeV
Y-90	Yttrium	2.6d	Beta	2,27 MeV
Lu-177	Lutetium	6.7d	Beta Gamma	498KeV 208KeV
Ra-223	Radium	11.4d	Alpha	

Quantitative imaging of radionuclide therapy isotopes is challenging

Most isotopes are only emitting beta or gammas of high energies

Radiation Dosimetry Aspects of 177Lu, Current Radiopharmaceuticals, 8(2): 139-144. Michael Lassmann and Uta Eberlein

Imaging therapeutic radionuclides

Indirect methods

1. Sister 'imaging' isotope

I-131 ←→ I-123 (SPECT)
I-131 ←→ I-124 (PET)
Y-90 ←→ Y-86 (PET)

2. Another 'imaging' isotope On same molecule

Y-90←→ In-111 (SPECT)

+ Good image quality
- More expensive
- Distribution may be different
- Halflife need to match

Direct methods

3. Additional gamma or positron of therapeutic isotope

Lu-177→ 208 keV (SPECT)
I-131 → 364 keV (SPECT)

4. Secondary Brehmstrahlung photons generated by β^- particle

Y-90

+ Therapeutic Distribution
- image quality

How to obtain the image for dose calculations?

Radionuclide		t1/2	emission	EMax	Option
I-131	Iodine	8d	Beta Gamma	606KeV 365 KeV	1 or 3
Y-90	Yttrium	2.6d	Beta	2,27 MeV	1 or 4
Lu-177	Lutetium	6.7d	Beta Gamma	498KeV 208KeV	2
Ra-223	Radium	11.4d	Alpha		?

Focus on imaging high energy

Imaging Y-90 with conventional gamma camera

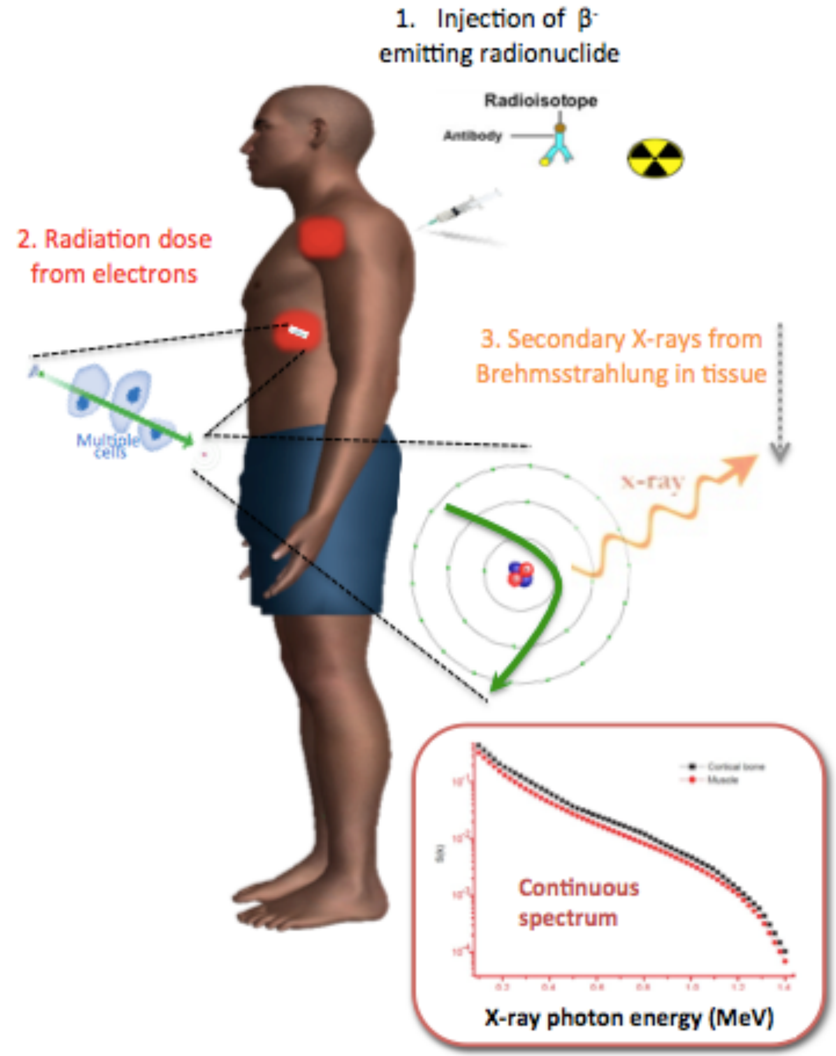

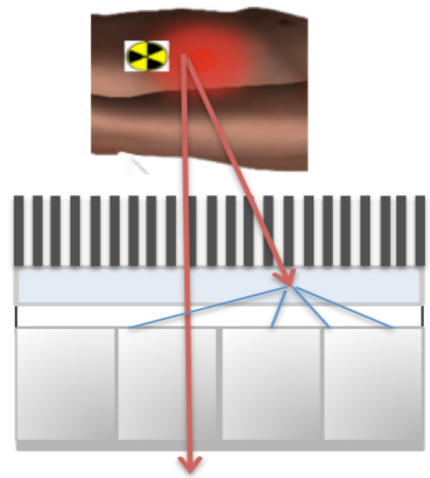

High energy
→ Penetration of collimator
→ Low detection efficiency

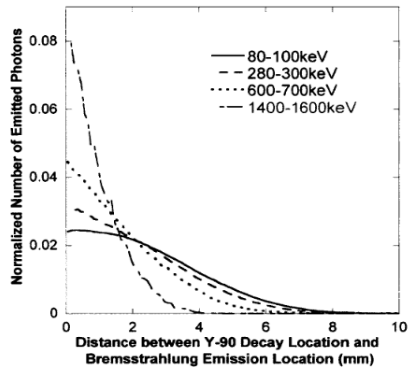

PhD, E. Rault Ugent PhD, X.Rong, University Baltimore, E.Frey

High energy peaks lead to contamination in main energy window

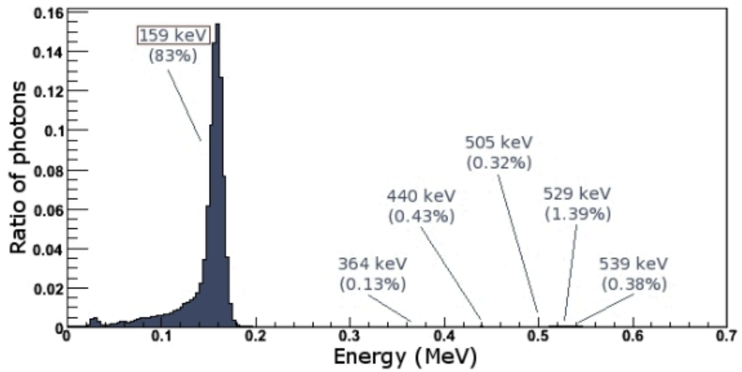

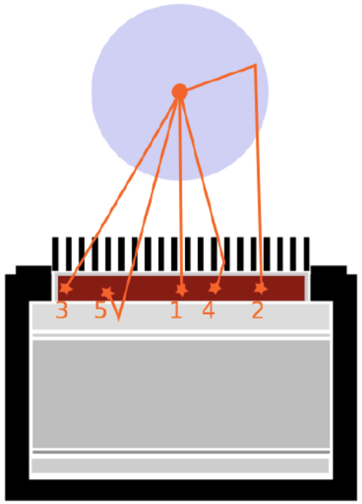

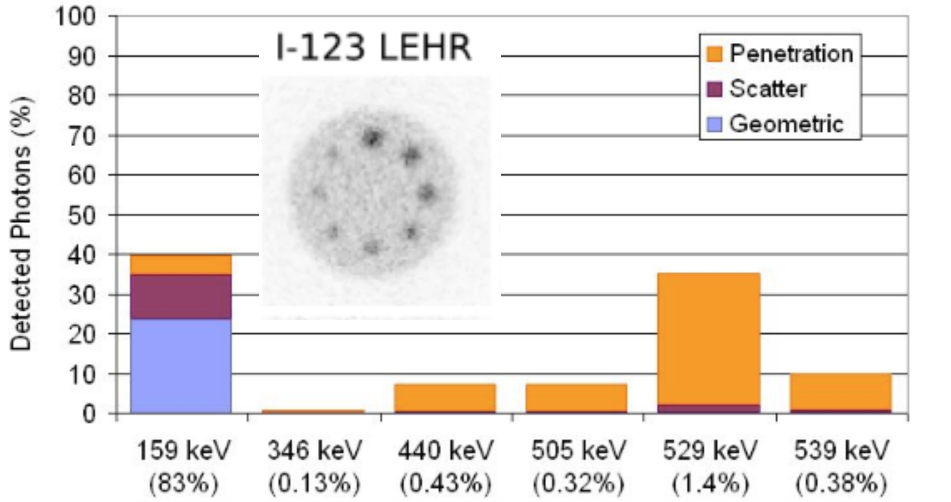

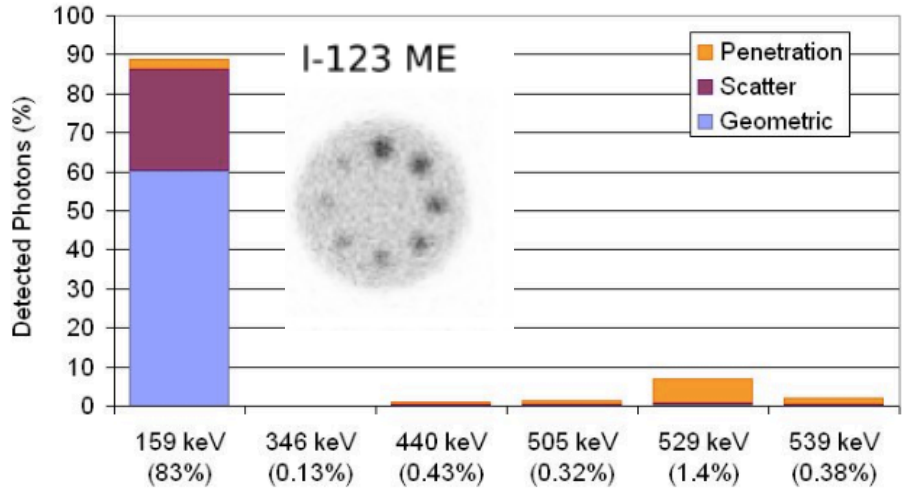

Comparison of image quality of different iodine isotopes (I-123, I-124 and I-131)

Erwann Rault, Stefaan Vandenberghe, Roel Van Holen, Jan De Beenhouwer, Steven Staelens, and Ignace Lemahieu

Collimator choice on gamma camera

Spectrum Y-90

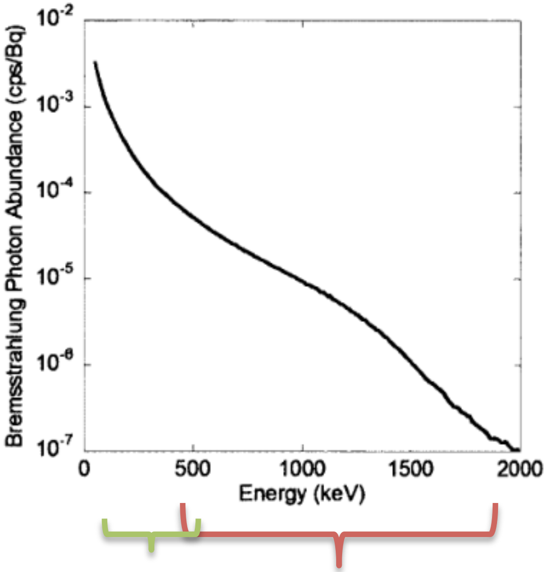

Geometric
with sensitivity
+ resolution

Penetration of
collimator
downscatter

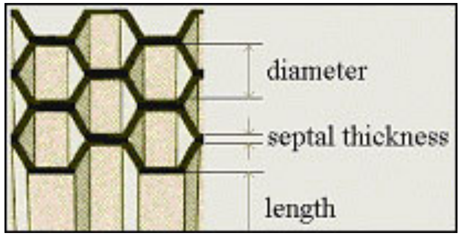

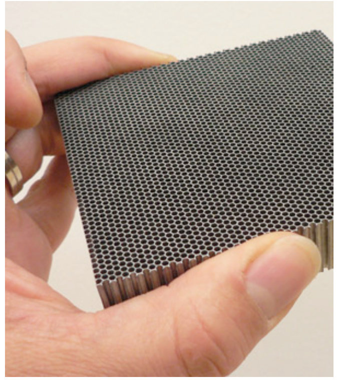

High
energy

Medium
energy

Low
energy

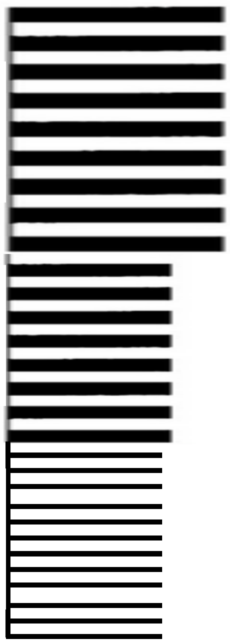

Low Penetration

Poor spatial
resolution

Best
choice

Good spatial
resolution

High Penetration

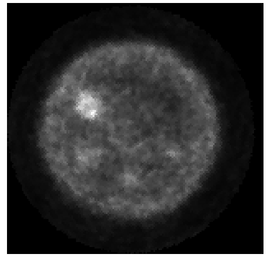

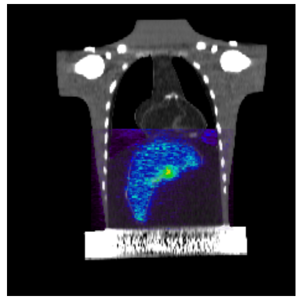

Comparison of yttrium-90 SPECT and PET images, Erwann Rault, Enrico Clementel, Stefaan Vandenberghe, Yves D'Asseler, Roel Van Holen, Jan De Beenhouwer and Steven Staelens J Nucl Med. 2010; 51 (Supplement 2):125

Y-90 has also a very low positron fraction: PET and TOF-PET

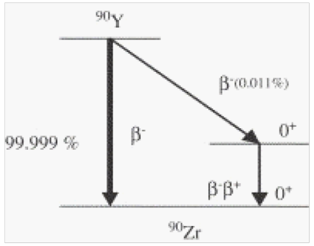

Very low sensitivity
32 positrons/MBq

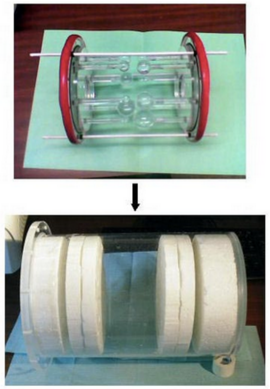

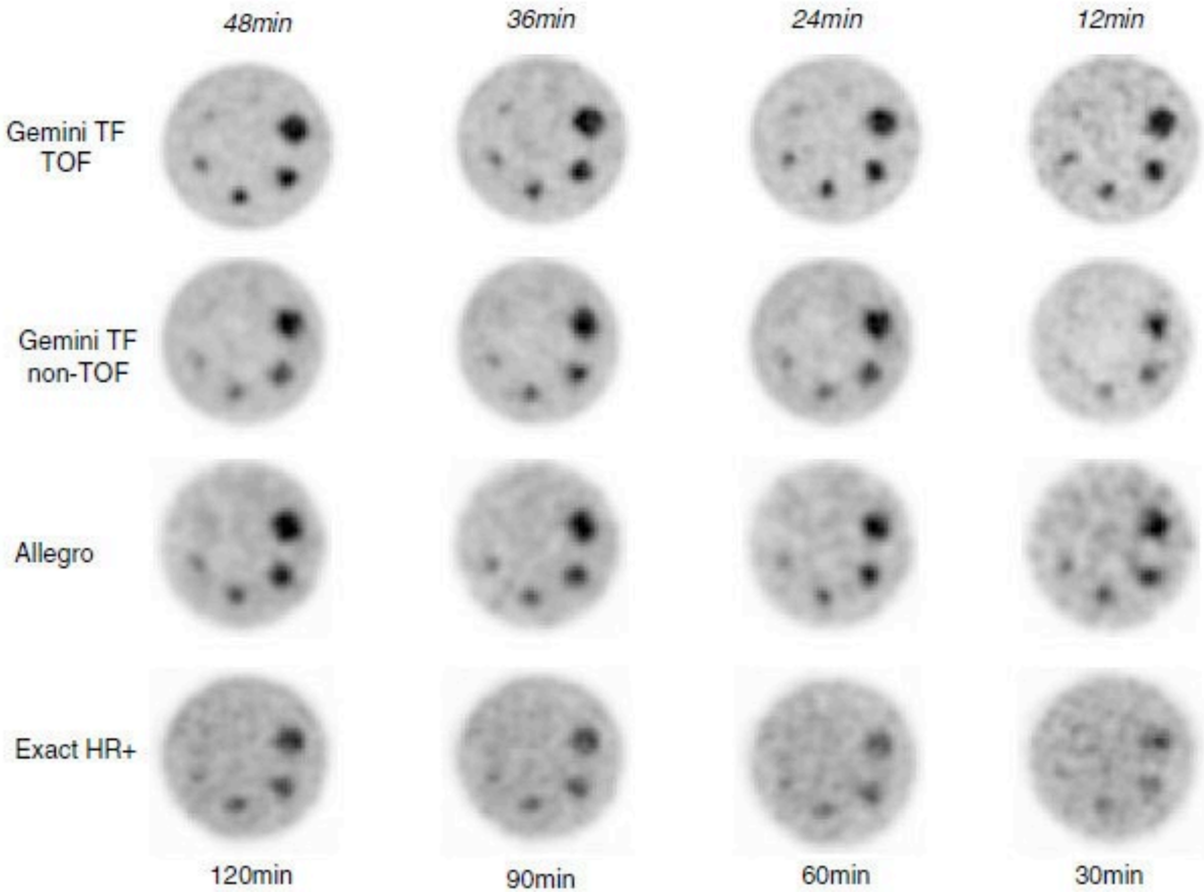

Comparison of yttrium-90 quantitative imaging by TOF and non-TOF PET in a phantom of liver selective internal radiotherapy. van Elmbt L1, Vandenberghe S, Walrand S, Pauwels S, Jamar F. Phys Med Biol. 2011 Nov 7;56(21):6759-77

Y-90
SPECT with ME versus PET

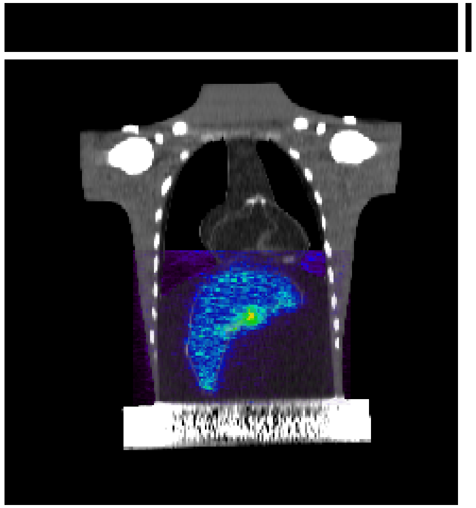

ME-SPECT

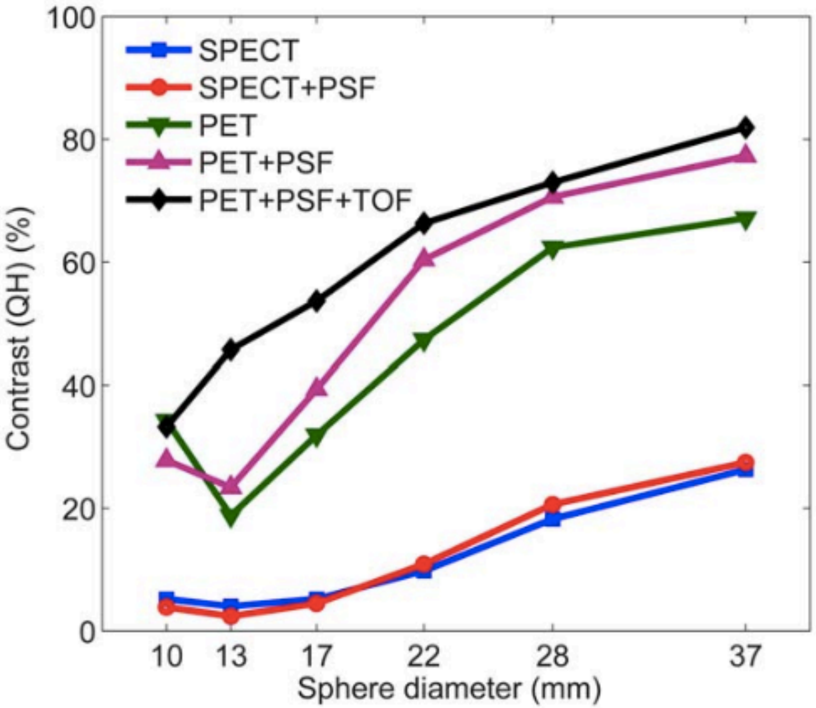

Quantitative comparison of PET and Bremsstrahlung SPECT for imaging the in vivo yttrium-90 microsphere distribution after liver radioembolization. Elschot M, Vermolen BJ, Lam MG, de Keizer B, van den Bosch MA, de Jong HW, Plos One 2013;8(2):e55742

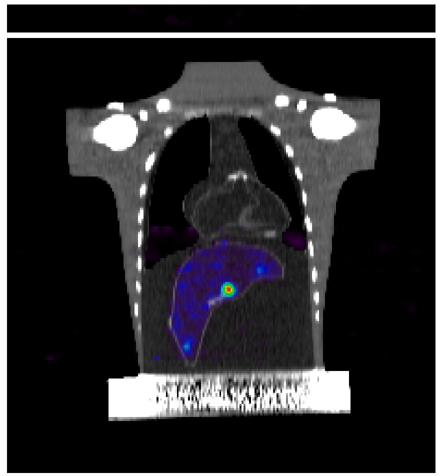

PET

Reasonable counts

Moderate spatial resolution

Low quantitative accuracy

Low counts

Good spatial resolution

Quantitative accuracy

Comparison of yttrium-90 SPECT and PET images, Erwann Rault, Enrico Clementel, Stefaan Vandenberghe, Yves D'Asseler, Roel Van Holen, Jan De Beenhouwer and Steven Staelens J Nucl Med. 2010; 51 (Supplement 2):125

Pinhole SPECT of high energy photons

I-131 (364 keV) imaging

On different Parallel hole collimators

High Penetration ⟷ Poor spatial resolution

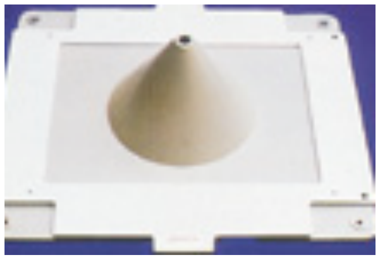

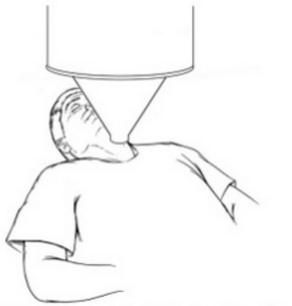

Pinhole design can be optimized
For penetration and resolution

511 keV singles imaging

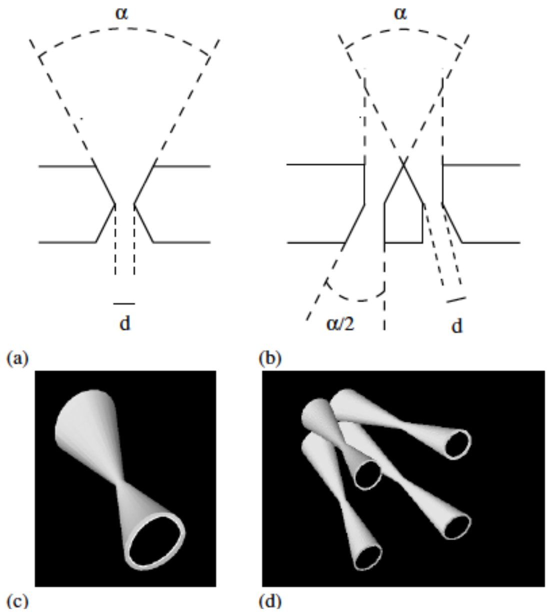

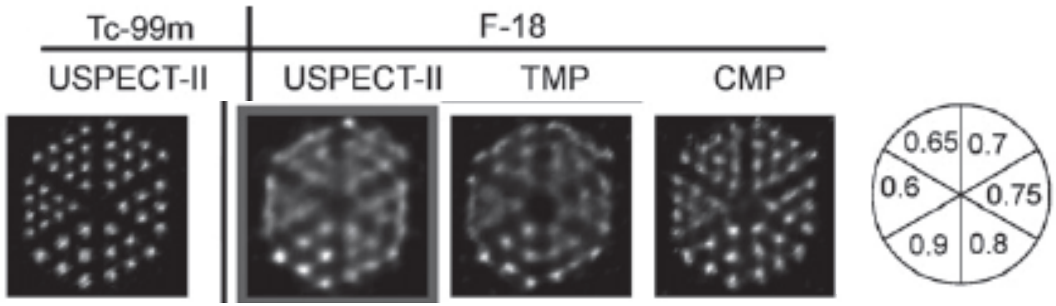

High-resolution tomography of positron emitters with clustered pinhole SPECT ,Marlies C Goorden and Freek J Beekman, Phys. Med. Biol. 55 (2010) 1265–1277

UCL Université catholique de Louvain

Y-90 with pinhole

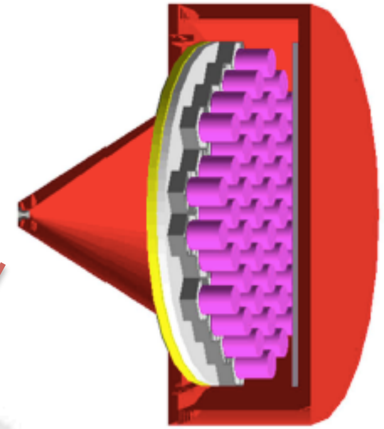

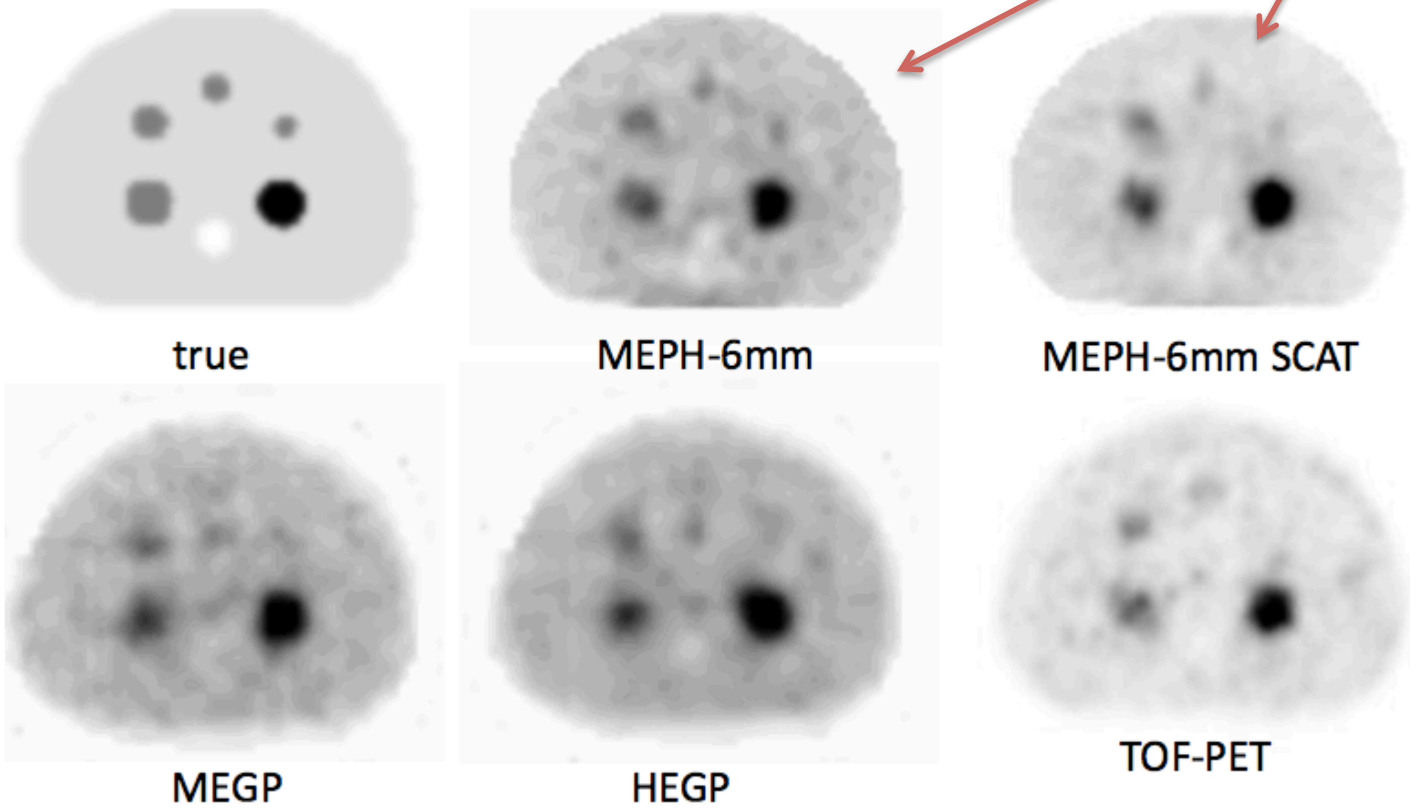

Yttrium-90-labeled microsphere tracking during liver selective internal radiotherapy by *bremsstrahlung* pinhole SPECT: feasibility study and evaluation in an abdominal phantom

Stephan Walrand[1*], Michel Hesse[2], Georges Demonceau[2], Stanislas Pauwels[1] and François Jamar[1]

EJNMMI Research
a SpringerOpen Journal

How to image bremsstrahlung efficiently ?

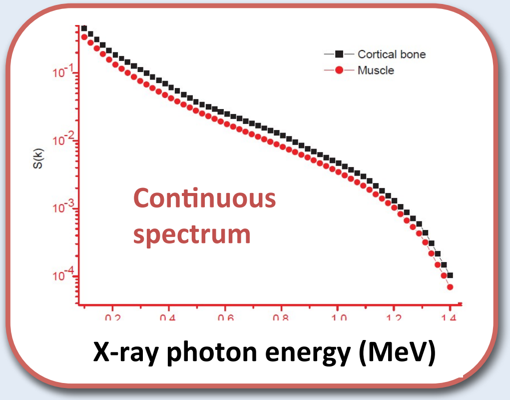

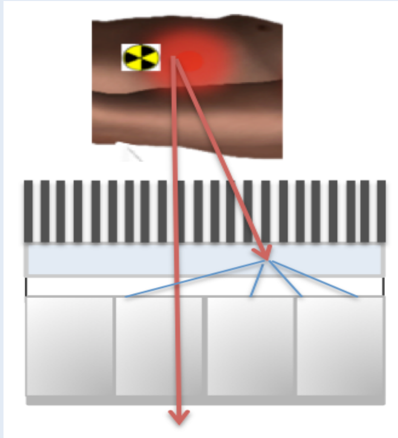

→ Penetration of collimator
→ Low detection efficiency

Improved Collimation

Pinhole Collimation of low and high energy X-rays

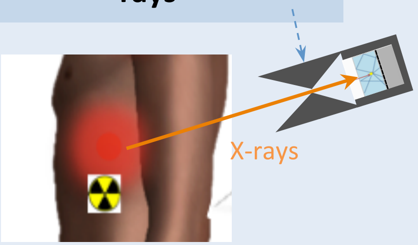

Improved detectors

Higher stopping power at low cost

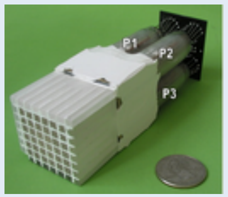

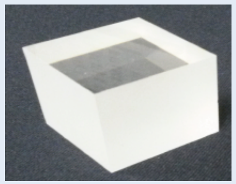

BGO system with pinhole collimator

3/8 inch NaI

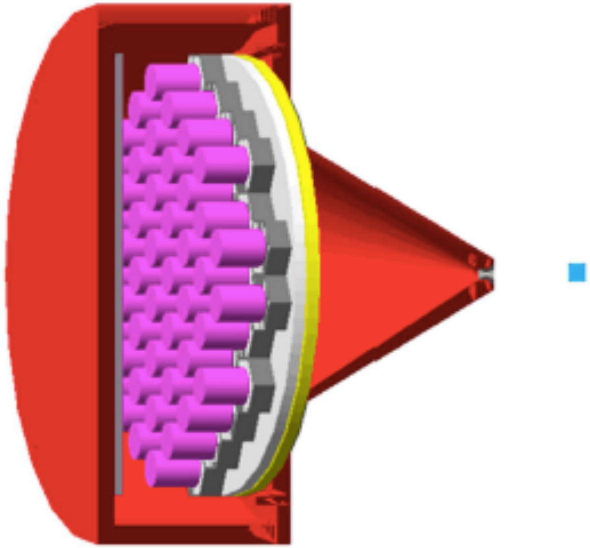

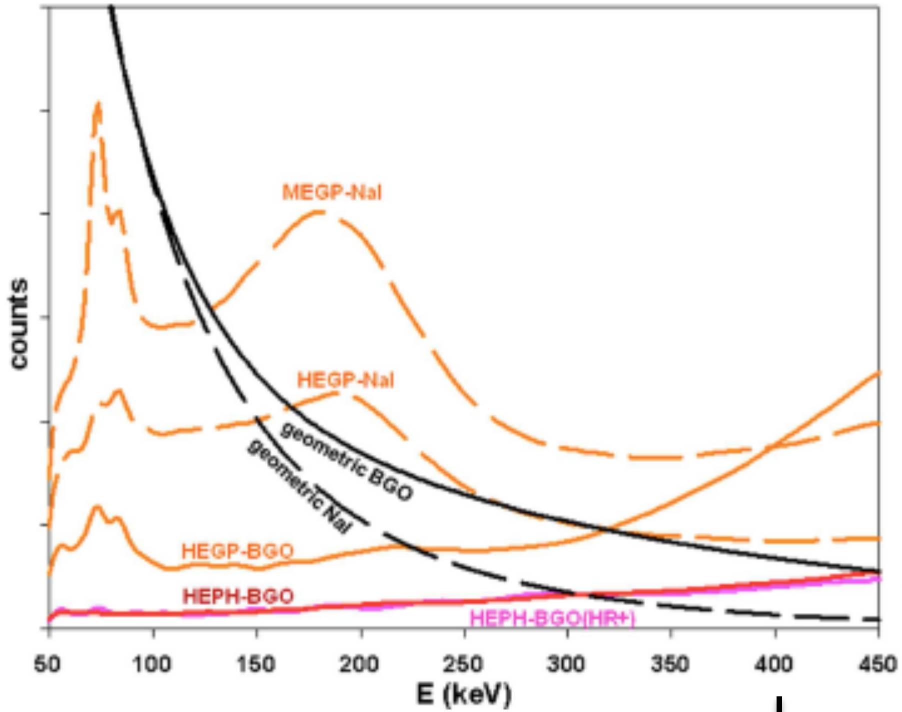

Reduction in Scatter contribution from ME to HE to pinhole collimator

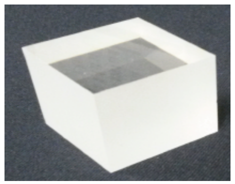

30 mm thick BGO

At 400 keV BGO captures 4.8 more geometric photons than NaI

Optimal design of Anger camera for bremsstrahlung imaging: Monte Carlo evaluation
StephanWalrand, Michel Hesse, Randy Wojcik , Renaud Lhommel and François Jamar
Frontiers in oncology, 2014

Continuous-spectrum emission tomography

Injection of radioactive labelled molecule for delivering internal radiation

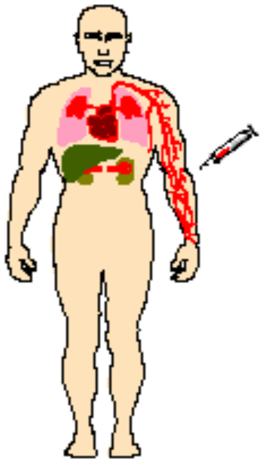

Continous spectrum of secondary radiation from electrons

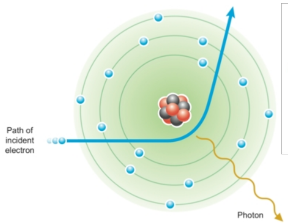

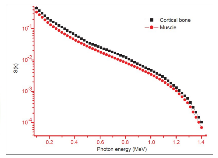

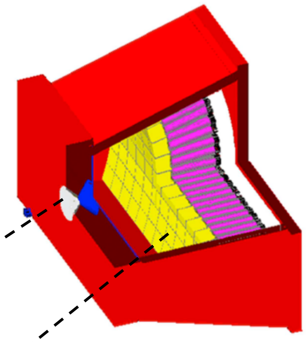

Collimation of low and high energy photons 50-1000 keV

Thick detector 50-1 MeV

Rotation over 180 deg

Monte Carlo based Reconstruction

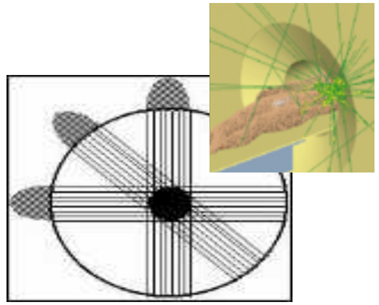

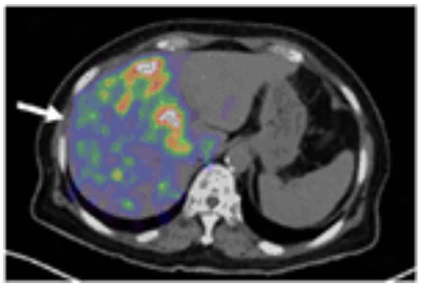

Dosimetry

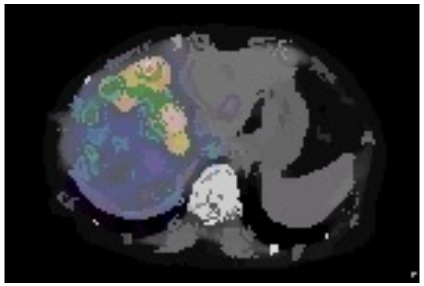

Feedback to therapy

Courtesy: Stefaan Vandenberghe, Medisip-Ugent-Iminds, Stephan Walrand, UCL

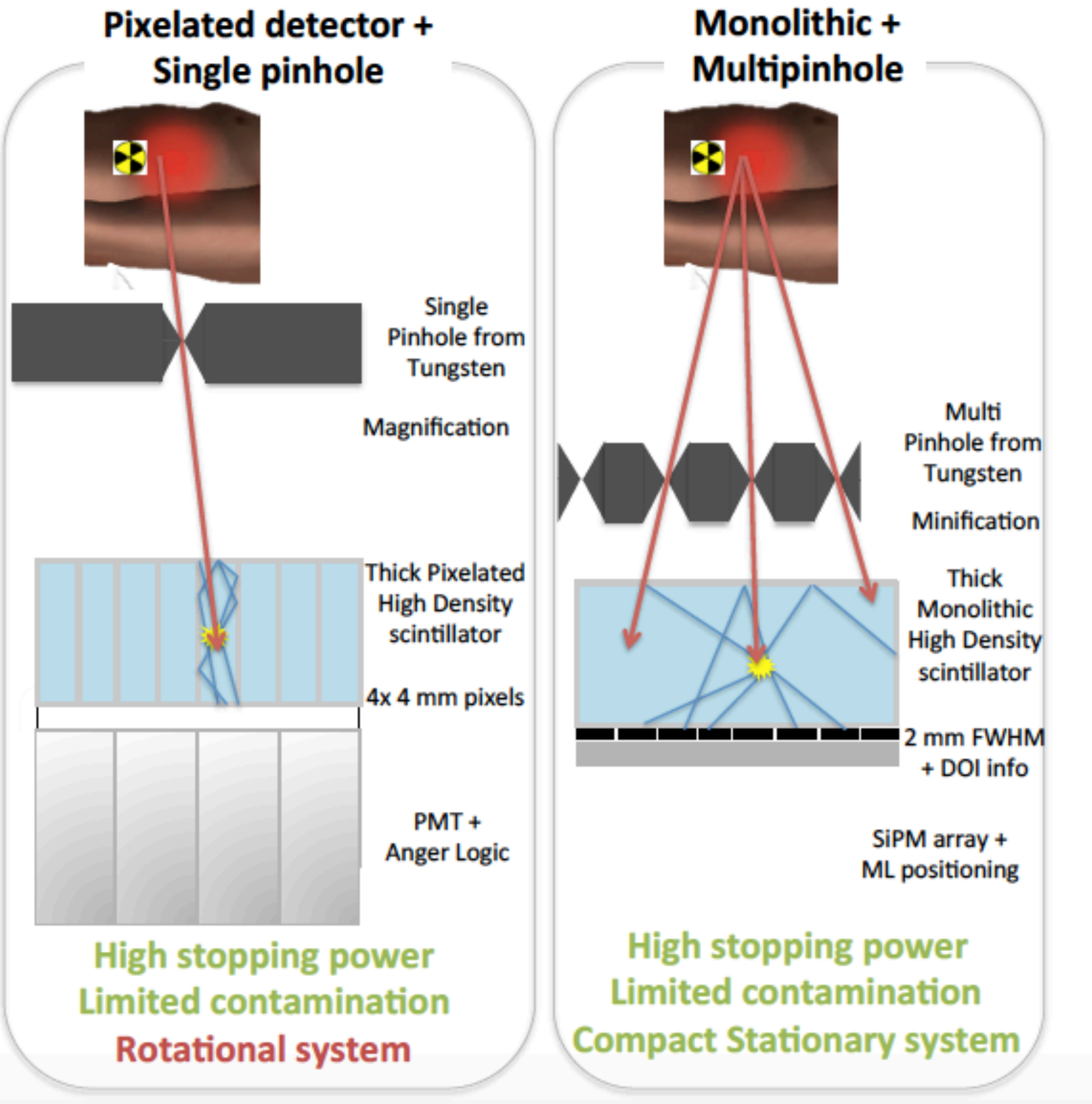
Pixelated detector + Single pinhole
Single Pinhole from Tungsten
Magnification
Thick Pixelated High Density scintillator
4x 4 mm pixels
PMT + Anger Logic
High stopping power
Limited contamination
Rotational system
Monolithic + Multipinhole
Multi Pinhole from Tungsten
Minification
Thick Monolithic High Density scintillator
2 mm FWHM + DOI info
SiPM array + ML positioning
High stopping power
Limited contamination
Compact Stationary system

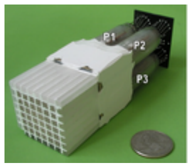
P1
P2
P3

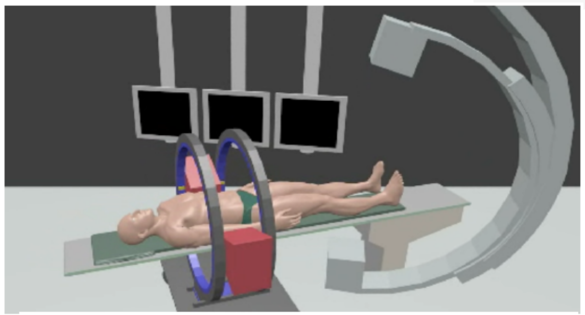

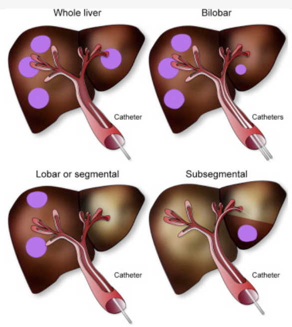
Whole liver
Bilobar
Catheter
Catheters
Lobar or segmental
Subsegmental
Catheter
Catheter

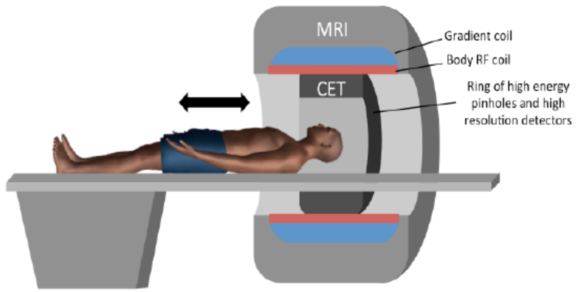
MRI
CET
Gradient coil
Body RF coil
Ring of high energy pinholes and high resolution detectors

High density monolithic BGO block (3.2.x3.2 x 3 cm)

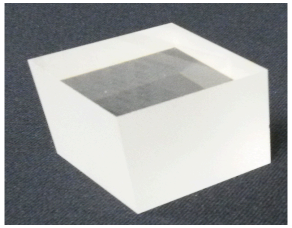

Spectrum of all detected counts

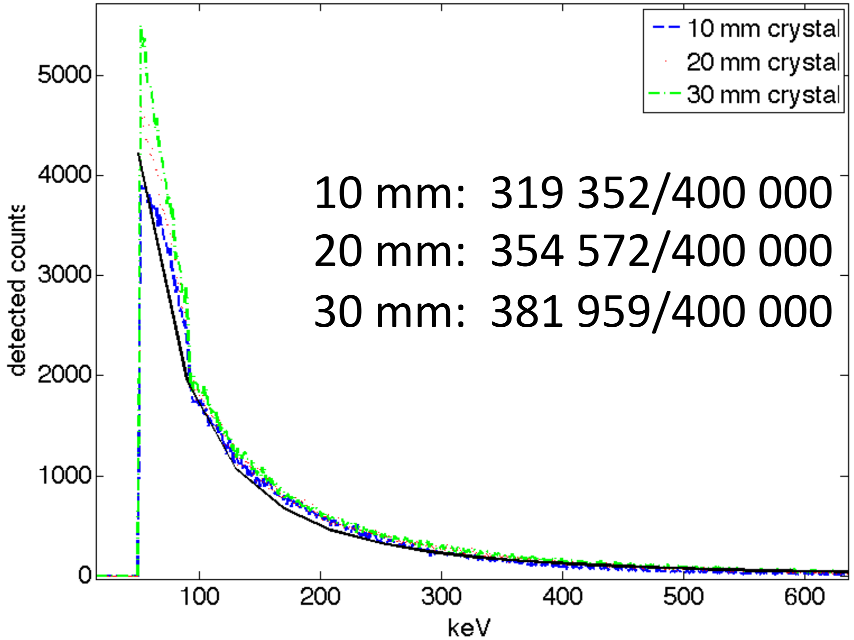

Macro (Gate) from previous study was adapted

- Collimator was removed
- Beam source perpendicular on detector

- Simulated 3 thicknesses of BGO: 10, 20 and 30 mm with Gate V6.1.
- Input: Brehmsstrahlung emission spectrum of Y-90 (4 kBq)

CS fraction at different energies

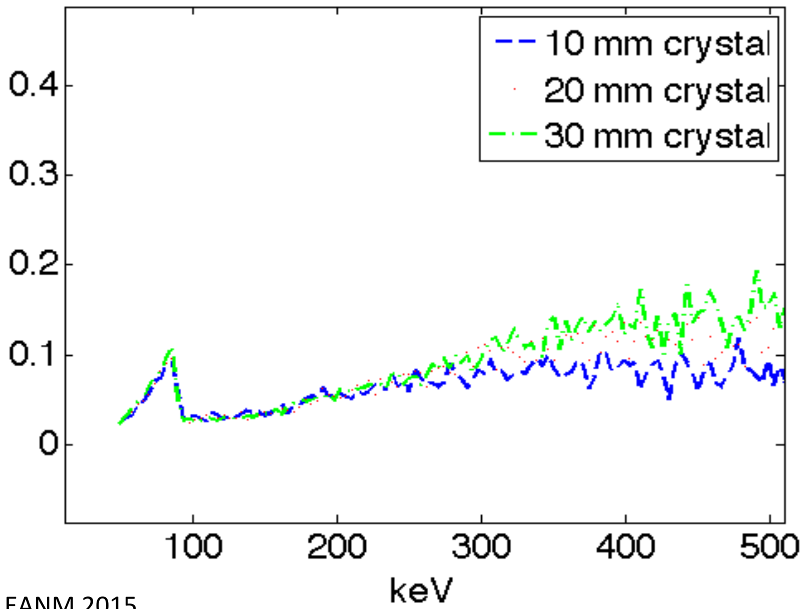

Continuous-spectrum Emission Tomography (CET) for quantifying the absorbed dose of in-vivo bremsstrahlung. **S. Vandenberghe**, H. W. A. De Jong, M. Bardies, D. Borys, M. de Jong, S. Walrand; EANM 2015

Monolithic BGO system with pinhole collimator

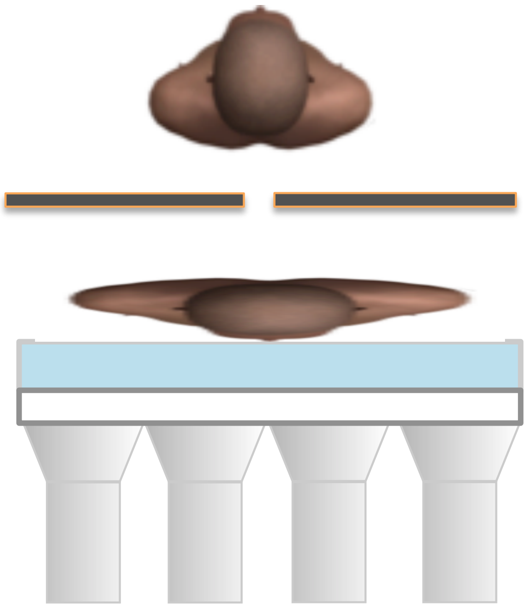

Systems with large detectors with 3 mm spatial resolution

Magnification

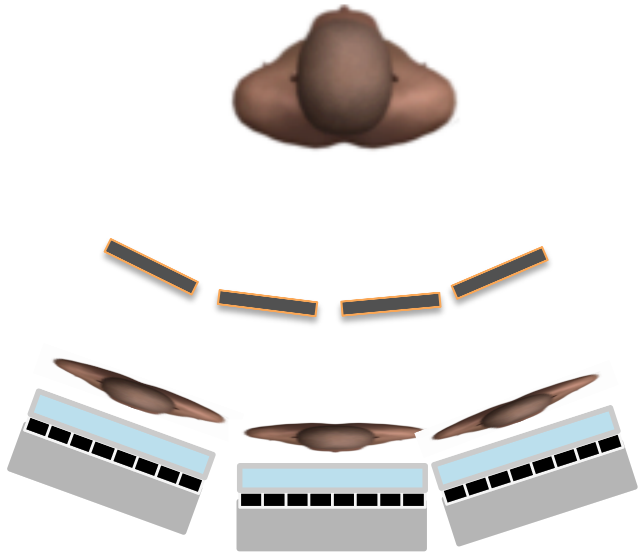

Systems with small detectors with

0.5-1 mm spatial resolution

Minification mode

More pinholes and stationary

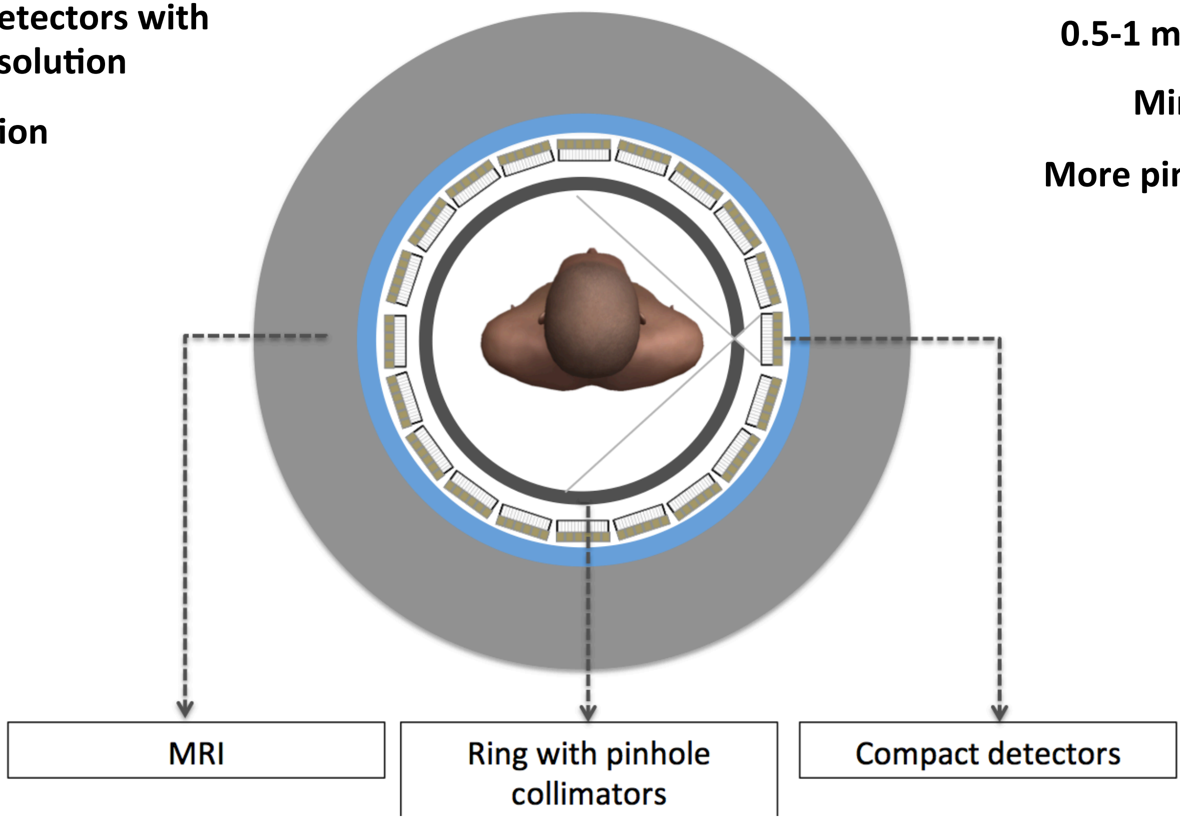

Design of Monolithic BGO system

Constraints

1. MR inner bore of 70 cm
2.Thickness of the detector 25 mm (10 mm BGO + 15 mm for readout)
2. Intrinsic spatial resolution of 1.5 mm
3. 10 mm spatial resolution in center of FOV
4. Pinhole sees 45 cm of object in center

The combination of a collimator opening of 1.15 mm with minification of 4.9 results in 22 pinholes per ring and 22 subdetectors of 9.2 cm

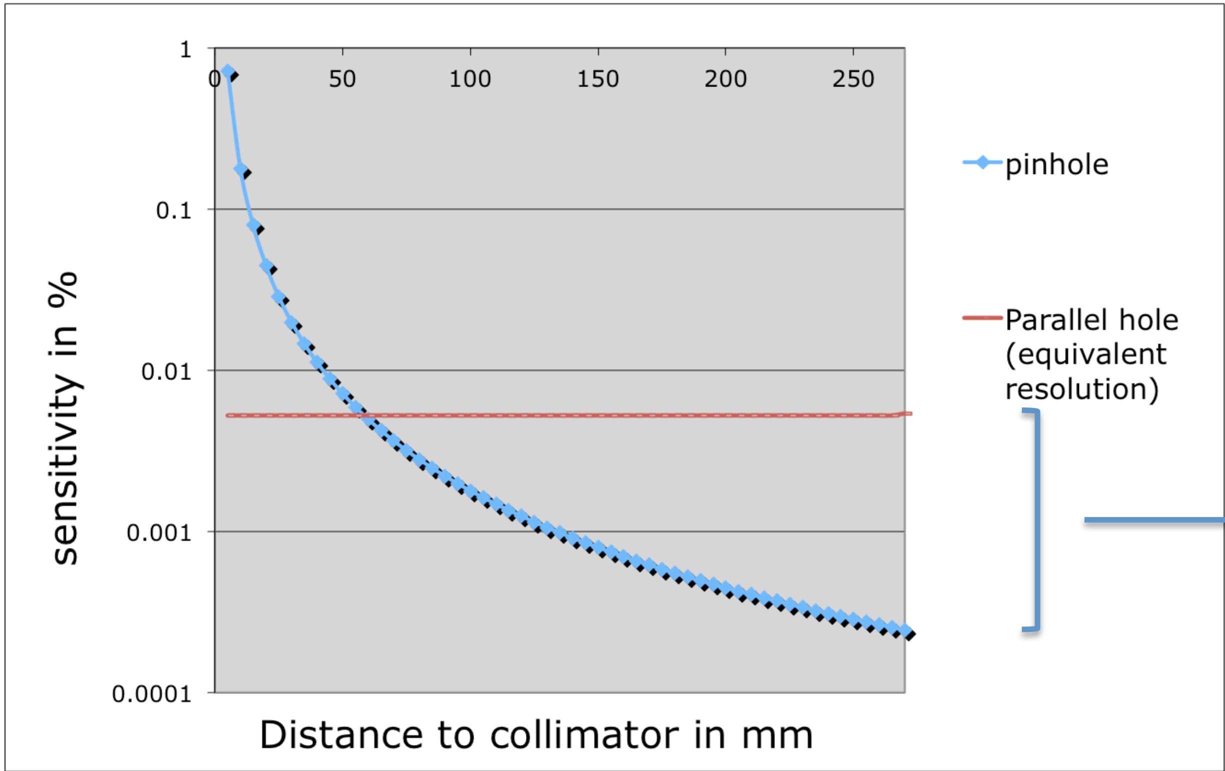

Ratio of sensitivities in center is 20.5

Summary

Several options for imaging therapeutic radionuclides

System with BGO and pinhole hasmuch higher efficiency than current SPECT or PET systems

A 10 mm monolithic BGO is a good compromise between detection efficiency, scatter fraction and spatial resolution

Based on these detectors a stationary system can be designed with 1 cm spatial resolution in the cFOV

EANM'16

Barcelona, Spain

Annual Congress of the
European Association of Nuclear Medicine

October 15 – 19, 2016
Barcelona, Spain

Pre-symposium @ EANM 2016 organized by EANM Physics committee

"Imaging for radionuclide therapy with statistical SPECT/PET reconstruction"
Saturday 15 october

Questions ?

MEDISIP

medisip.elis.ugent.be

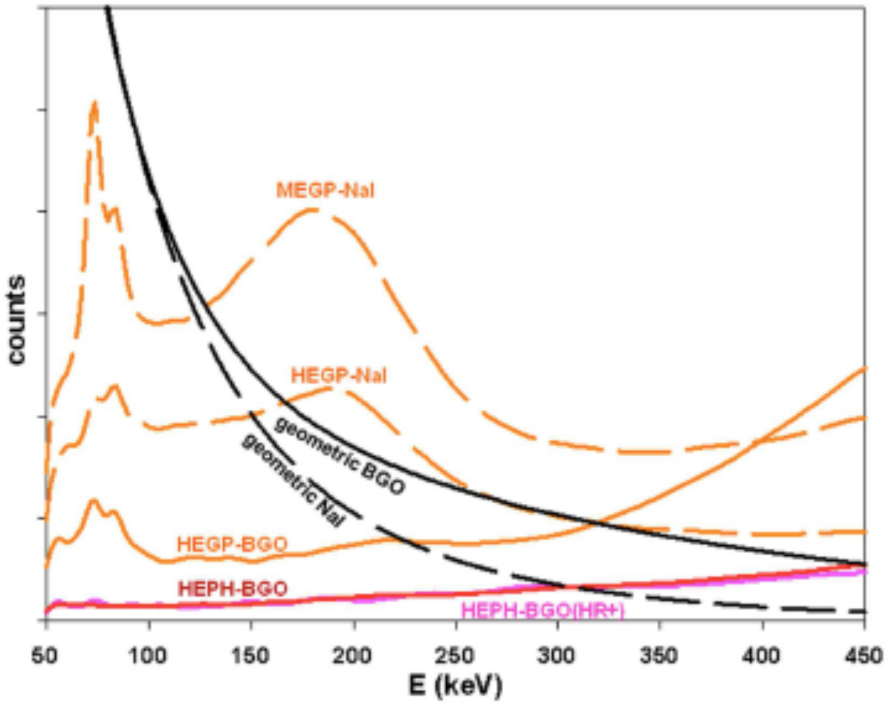

FIGURE 5 | Comparison of the total scatter components (colored curves) with the geometric x-rays (black curves) obtained by MC simulations for a ^{90}Y point source surrounded by 1 cm of perpex and set 10 cm in front of the collimator. Septa thickness is 1.4 and 3.2 mm, hole diameter is 3.4 and 4.0 mm, hole length is 42 and 40 mm, for the MEGP and HEGP collimator, respectively. Front wall thickness of 5 cm, aperture diameter of 8 mm, focal length of 15 cm for the HEPH collimator. 45 cm × 25 cm crystal: 3/8"-thick NaI and 30 mm-thick BGO. The purple curve corresponds to the BGO prototype (see second last section). The BGO to NaI geometric ratio is 4.8 at 400 keV, which is in line with the 4.9 predicted by previous MC simulations (**Figure 4**).